

ELLIPSOMETRIC STUDIES OF ErMnO_3 SINGLE CRYSTALS*

G.-J. Babonas^a, J.-C. Grivel^b, A. R  za^{a,c}, and R. Girkantait  ^c

^a Semiconductor Physics Institute, A. Go  tauto 11, LT-01108 Vilnius, Lithuania

E-mail: jgb@pfi.lt

^b Materials Research Department, Ris   National Laboratory, Technical University of Denmark, DK-4000 Roskilde, Denmark

^c Faculty of Physics and Technology, Vilnius Pedagogical University, Studentų 39, LT-08106 Vilnius, Lithuania

Received 8 June 2007

Ellipsometric studies of ErMnO_3 single crystals have been carried out in the spectral range of 1–5 eV by means of photometric ellipsometers. Experimental ellipsometric data were analysed in the uniaxial crystal model. For the first time, the components of dielectric function of ErMnO_3 were determined. The fine structure of dielectric function spectra was analysed and the origin of the optical features was discussed taking into account the possible mechanisms of electronic excitations. It was shown that intra-configuration optical transitions of $d-d$ and $f-f$ types in Mn^{3+} and Er^{3+} ions, respectively, and charge-transfer transitions $\text{O}(2p) \rightarrow \text{Mn}(3d)$ contribute to the optical response of ErMnO_3 . The optical spectra and electronic energy band structure of ErMnO_3 was compared with those for other manganites.

Keywords: manganites, optical properties, electronic energy band structure

PACS: 75.47.Lx, 78.20.-e

1. Introduction

Undoped RMnO_3 ($R = \text{La, Nd, Pr, Er}$) and doped $\text{R}_{1-x}\text{A}_x\text{MnO}_3$ ($A = \text{Ca, Sr, Ba}$) manganites [1] have attracted a lot of attention due to their colossal magnetoresistance. The double exchange model was used to explain the ferromagnetism and metallicity of manganites. Two additional models were developed for the interpretation of colossal magnetoresistance. The models take into account the polarons due to Jahn–Teller effect for Mn^{3+} ions and the orbital fluctuations. In order to determine the microscopic mechanism of these phenomena, the optical properties of manganites were studied along with magnetic interactions.

The structural difference between LnMnO_3 (Ln is a lanthanide) compounds should be emphasized. On the one hand, manganites containing large ionic radius lanthanides (La, Ce–Dy) crystallize in a distorted orthorhombic perovskite structure [1]. On the other hand, manganites with small ionic radius lanthanides (Ho–Lu) crystallize in a hexagonal structure. The coordination polyhedra for Mn differ in crystal lattices of various symmetry leading to different physical properties of manganites. While manganites with perovskite

structure possess a colossal magnetoresistance effect, manganites of hexagonal symmetry are of interest because of the combination of ferroelectric and magnetic ordering [2]. In order to reveal the correlation between crystal structure and electronic energy band structure of manganites, the optical spectra of compounds from two groups, e. g., NdMnO_3 [3] and ErMnO_3 , are to be compared.

The optical properties of ErMnO_3 were not widely investigated. Nonlinear optical spectroscopy and Faraday rotation were studied in [4]. In the present work, ellipsometric studies of ErMnO_3 have been carried out and the mechanism of the electronic transitions responsible for corresponding optical features is discussed.

2. Experimental

The ErMnO_3 single crystals were grown in Ris   National Laboratory by means of the travelling solvent floating zone (TSFZ) technique. The starting reagents, MnO_2 and Er_2O_3 powders (Alfa Aesar, 99.9% purity), were mixed in ethanol and dried under stirring. After calcination at 900   C in air, the powders were mixed with polyvinyl alcohol that acted as a binder. Rods were isostatically pressed and sintered at 1350   C in air in a vertical furnace. After sintering, the rods had

* The report presented at the 37th Lithuanian National Physics Conference, 11–13 June 2007, Vilnius, Lithuania.

a diameter of about 8 mm and a length of 3 cm (seed) and 9 cm (feed). The composition of the feed rod was $\text{ErMn}_{1.01}\text{O}_x$ to compensate for Mn evaporation from the melt during the growth process. The growth was performed in flowing air in a mirror furnace (Crystal Systems Inc) equipped with 4 lamps of 1500 W maximum power. The molten zone was moved upwards at a rate of 5 mm/h, while the rods were counter rotated at 25 rpm.

The XRD analysis of obtained ErMnO_3 single crystals was performed. From the Laue diffraction pattern, a hexagonal symmetry, the space group $P6_3cm$, and lattice parameters $a = 6.117 \text{ \AA}$ and $c = 11.435 \text{ \AA}$ were determined. The unit cell contains six formula units. In hexagonal lattice Er^{3+} ions are located in $2a$ positions (local symmetry $3m$) and $4b$ sites (symmetry 3). Magnetic Mn^{3+} ($3d^4$) ions occupy $6c$ positions (symmetry m) coordinated by O^{2-} ions. The structural parameters were in a good agreement with previous structural data [5].

The characteristic structural units in ErMnO_3 cell are Mn–O and Er–O polyhedra. The Mn ions are situated in a trigonal bipyramid (Fig. 1(a)), which is sharing the corners with neighbouring Mn–O polyhedra. The ordering of polyhedra results in a two-dimensional nature of the structure. The distance from Mn atom to the nearest five O atoms varies from ~ 1.85 to $\sim 2.09 \text{ \AA}$ [5] and it is shortest to apical O atoms and longest for the bonds in the basal plane. The striking structural anisotropy for in-plane and out-of-plane Mn–O bond lengths is a particular feature of ErMnO_3 lattice as compared to that of NdMnO_3 [6]. In NdMnO_3 the Mn–O distance is largest for apical O atoms in MnO_6 octahedron. In ErMnO_3 both Er atoms are eightfold coordinated with polyhedron in the shape of distorted bicapped trigonal antiprism (Fig. 1(b)). Both Er–O polyhedra are similar in shape though 180° -rotated around b axis with respect to each other. The distortion of Er–O polyhedra is responsible for ferroelectric properties of ErMnO_3 [2]: dipole moments of four $\text{Er}(2)$ –O polyhedra are antiparallel to those of two $\text{Er}(1)$ –O polyhedra resulting in a ferrielectric configuration.

Several samples with polished surfaces were prepared for optical studies. In ellipsometric measurements, the surface of area $3 \times 8 \text{ mm}^2$ was used with the c axis oriented along the short side of the sample. The optical transmission measurements have been carried out on the platelet of 1.2 mm thickness and $\varnothing 6 \text{ mm}$ with c axis in the surface plane.

Two spectroscopic ellipsometers were used, a standard SOPRA GES5 ellipsometer with rotating polar-

izer and home-made photometric ellipsometer with rotating analyzer. In the latter case, the ellipsometric parameters were determined with $\sim 0.02^\circ$ accuracy. The systematic errors due to wandering of light spot on the photomultiplier cathode and nonlinearity of the detector response were taken into account. The ellipsometric data were obtained in the spectral range of 1–5 eV. The complex reflectivity ρ was determined from ellipsometric measurements

$$\rho = \frac{r_{\parallel}}{r_{\perp}} = \tan \Psi \exp(i\Delta), \quad (1)$$

where r_{\parallel} and r_{\perp} are Fresnel coefficients for light polarized parallel and perpendicular to the plane of light incidence, Ψ and Δ are ellipsometric parameters.

Two independent components $\varepsilon_x = \varepsilon_y = \varepsilon_o$ and $\varepsilon_z = \varepsilon_e$ of complex dielectric function $\varepsilon = \varepsilon_1 + i\varepsilon_2$ (where $\varepsilon_1 = \text{Re}(\varepsilon)$ and $\varepsilon_2 = \text{Im}(\varepsilon)$) for ErMnO_3 were determined in the uniaxial crystal model. Two experimental runs of the measurements were carried out in order to obtain two pairs of Fresnel coefficients:

$$r_{\parallel} = \frac{\sqrt{\varepsilon_o \varepsilon_e} \cos \theta - \sqrt{\varepsilon_o - \sin^2 \theta}}{\sqrt{\varepsilon_o \varepsilon_e} \cos \theta + \sqrt{\varepsilon_o - \sin^2 \theta}},$$

$$r_{\perp} = \frac{\cos \theta - \sqrt{\varepsilon_o - \sin^2 \theta}}{\cos \theta + \sqrt{\varepsilon_o - \sin^2 \theta}} \quad (2)$$

for c axis in the incidence plane and

$$r_{\parallel} = \frac{\varepsilon_o \cos \theta - \sqrt{\varepsilon_o - \sin^2 \theta}}{\varepsilon_o \cos \theta + \sqrt{\varepsilon_o - \sin^2 \theta}},$$

$$r_{\perp} = \frac{\cos \theta - \sqrt{\varepsilon_e - \sin^2 \theta}}{\cos \theta + \sqrt{\varepsilon_e - \sin^2 \theta}} \quad (3)$$

for c axis perpendicular to incidence plane. In (2) and (3) θ is the angle of light incidence, which has been equal to 70° in a typical ellipsometric run.

3. Results and discussion

Figure 2 presents the spectral dependence of dielectric function components of hexagonal ErMnO_3 . As is seen, a rich fine structure is observed in the optical spectra of ErMnO_3 . As in the other manganites [3], several main peaks are to be noted in the region of ~ 1.5 , 2.2 , and 3.4 eV . A particular feature of ErMnO_3 is a strong anisotropy of the peak at 1.5 eV . The

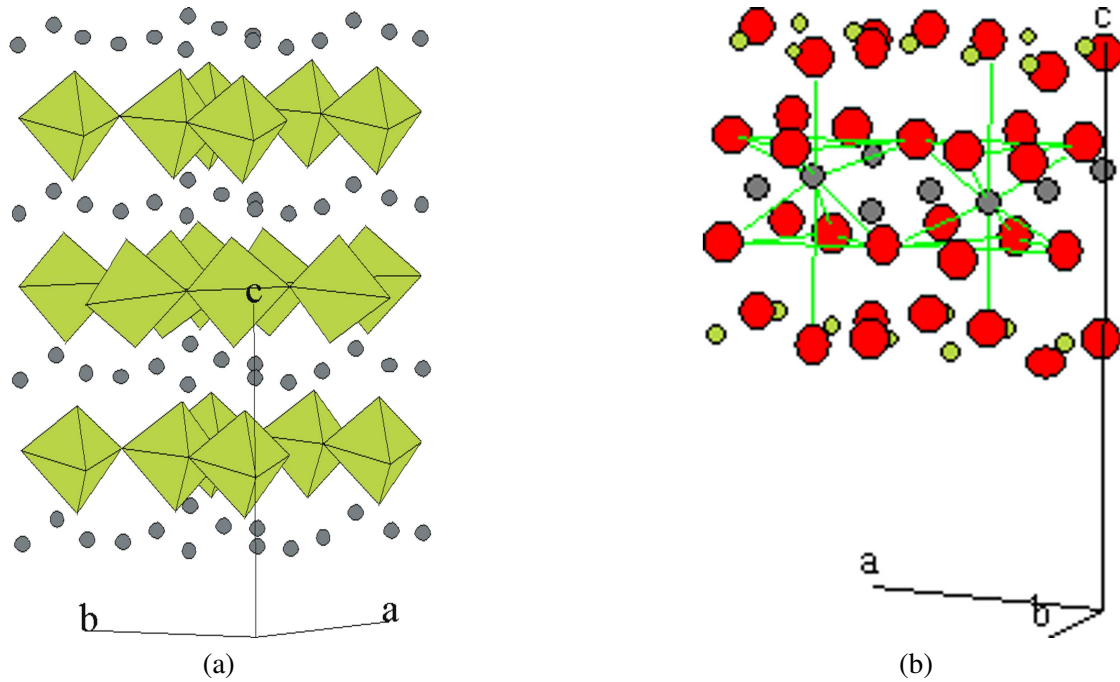


Fig. 1. (a) Mn–O and (b) Er–O polyhedra in the structure of hexagonal ErMnO₃. In (a) dark circles are Er atoms; in (b) small, middle, and big circles are Mn, Er, and O atoms, respectively.

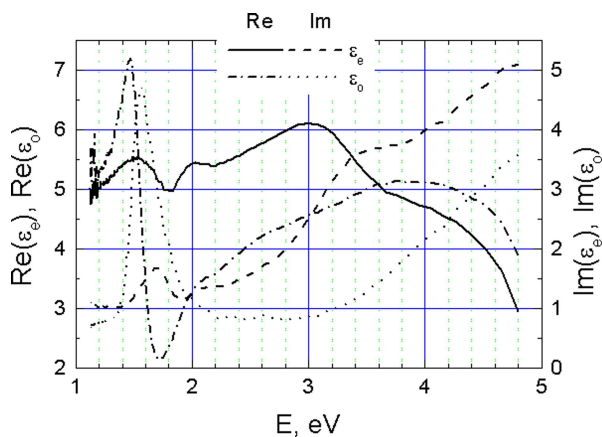


Fig. 2. Spectral dependences of the dielectric function components of hexagonal ErMnO₃.

fine structure in the spectral dependence of anisotropy (Fig. 3) is better resolved for anisotropy parameter

$$\Delta_{ac} = \frac{\varepsilon_{o2} - \varepsilon_{e2}}{\sqrt{\varepsilon_{o2}^2 + \varepsilon_{e2}^2}}. \quad (4)$$

In particular, as it follows from Fig. 3, at least two optical transitions at ~ 1.55 and 1.8 eV contribute to the main peak.

The edge of the fundamental absorption band is clearly seen from the absorption measurements of ErMnO₃ (Fig. 4). The constant refraction index $n = 2.4$ was assumed in the calculations of absorption coefficient. As is seen, the onset of absorption occurs at 1.4 – 1.5 eV and it is slightly different for polariza-

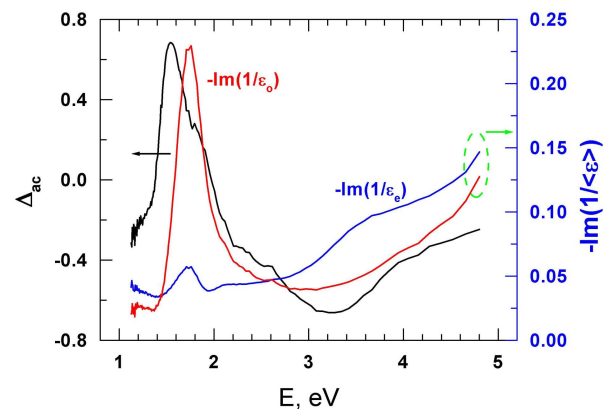


Fig. 3. Spectra of the parameter of anisotropy Δ_{ac} and energy loss functions $-\text{Im}(1/\varepsilon_i)$ (where $i = e, o$).

tions $e\parallel a$ and $e\parallel c$. Sharp absorption lines observed in the region of relative transmittance is unambiguously assigned to the f – f intra-configuration transitions in Er³⁺ (f^{11}) ions ($L = 6$ and $S = 3/2$). In accordance with the Er³⁺ spectra in various rare earth compounds [7], the series of lines at ~ 0.85 , 1.3 , and 1.55 eV are due to electronic excitations from the ground level $^4I_{15/2}$ to the excited multiplets $^4I_{13/2}$, $^4I_{11/2}$, and $^4I_{9/2}$, respectively. It is interesting to note that the structure of Stark-split components of multiplets is slightly different for two main light polarizations. A possible reason for this observation is occurrence of two non-equivalent Er sites in ErMnO₃. It is interesting to note that Faraday rotation was observed [4] in the region of

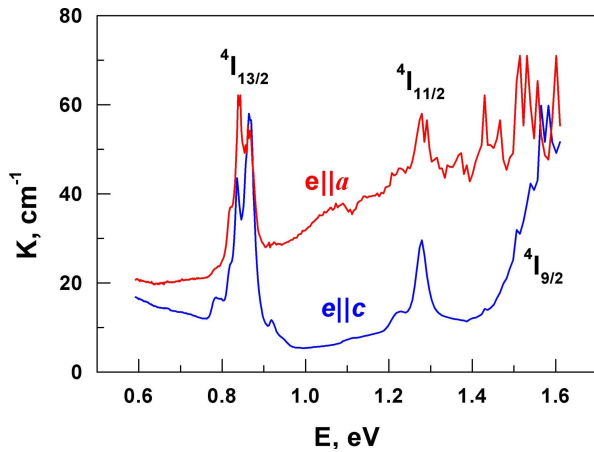


Fig. 4. Spectra of absorption coefficient $K(E)$ of ErMnO_3 for light polarized along the main directions of hexagonal lattice.

${}^4I_{15/2} \rightarrow {}^4I_{11/2}$ transitions along with a strong contribution of the electronic excitations in the fundamental absorption band with the resonance energy 1.67 eV, which is close to the low-energy peaks observed in the spectra of dielectric function (Fig. 2).

It is reasonable to analyse the fine structure of dielectric function spectra of manganites as a set of contributions originated from Lorentzian-like terms [3]. In this model, the energies of Lorentzian lines correspond to the electronic optical transitions between the levels in the energy scheme (see Fig. (5)).

The electronic energy band structure was analysed theoretically in several studies. In electronic structure of ferromagnet YMnO_3 [8] calculated in local density approximation, the absorption edge (at 1.1 eV) was attributed to charge transfer transitions. In the local spin-density approximation [9], the ferroelectromagnetic YMnO_3 was found to be a semiconducting compound with the band gap at 1.5 eV. It was also found [9] that the lowering of symmetry in hexagonal YMnO_3 is not connected with a Jahn–Teller instability, in contrast to perovskite manganites. In [4] the data on second harmonic spectroscopy on hexagonal manganites were interpreted by means of intraband dipole-allowed d – d transitions in the visible range. The onset of strong absorption at 1.3–1.5 eV in manganites was attributed to spin-allowed transitions within t_{2g} and e_g orbitals of Mn^{3+} ions split in local crystalline field of hexagonal manganites. These intraband transitions were assumed to have a high intensity because of acentric $6c$ positions of Mn^{3+} ions in the unit cell and their high concentration. Below, the ellipsometric data on ErMnO_3 will be considered in this approximation.

In hexagonal lattice, the crystal field symmetry ($\bar{6}m2$) of $\text{Mn}^{3+}(3d^4)$ ions situated in trigonal bipyra-

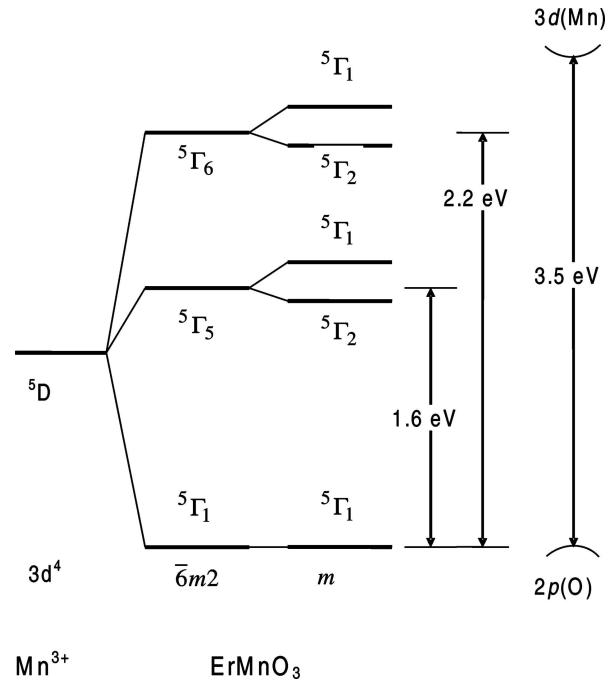


Fig. 5. Scheme of energy levels and optical transitions in ErMnO_3 (modified from [4]).

midal polyhedra causes the splitting of the 5D state into three components (Fig. 5), single 5G_1 ground state and two doubly degenerate excited states, 5G_5 (lower) and 5G_6 (higher) [9]. The d -type wave functions of the 5G_5 state are mixed with the p -type x and y wave functions [4]. As compared with the octahedral crystal field splitting Δ_o in perovskite manganites, in hexagonal manganites the overall splitting is $1.25\Delta_o$ with $0.87\Delta_o$ for ${}^5G_1 \rightarrow {}^5G_5$ and $0.38\Delta_o$ for ${}^5G_1 \rightarrow {}^5G_6$. A further splitting of the levels occurs in the low-temperature phase with a local symmetry m for $6c$ sites lifting degeneracy of 5G_5 and 5G_6 states. The charge transfer transitions $O(2p) \rightarrow \text{Mn}(3d)$ are assumed [4] to occur at $E > 3$ eV.

The experimental data (Figs. 2, 3) on ErMnO_3 are in a good agreement with the model described above. At first, the optical characteristics at ~ 1.6 eV are strongly polarized, the intensity being larger for $e||a$ in accordance to the predictions of the model. Therefore, they can be attributed to the ${}^5G_1 \rightarrow {}^5G_5$ transitions. Secondly, in this model the optical features at ~ 2.2 eV are assigned to the ${}^5G_1 \rightarrow {}^5G_6$ transitions. Thus, the energy gap 5G_6 – 5G_5 equals to 0.6 eV, the latter value agrees well with the crystal field splitting (0.7 eV) between these states estimated from the distance 5G_1 – 5G_5 . Thirdly, the mixing of p -type wave functions to 5G_5 state is most probably responsible for the high intensity of the peaks at 1.6 eV. Finally, the sign of the anisotropy parameter at 1.6 eV (Fig. 3) is opposite to that determined for peaks at 2.2 eV.

Comparison of optical spectra in ErMnO_3 and NdMnO_3 [3] reveals the general regularities and particular features of manganites of hexagonal and perovskite structure. The NdMnO_3 crystals of orthorhombic symmetry (space group $Pbnm$, $a = 5.4505 \text{ \AA}$, $b = 5.743 \text{ \AA}$, $c = 7.566 \text{ \AA}$ [3]) can be considered in the pseudo-cubic system because of a small crystal anisotropy along the a and b axes. Indeed, a slight difference in the localization of Mn–O polyhedra along the a and b axes causes a small optical anisotropy in the basal plane. Therefore, the spectrum of anisotropy parameter Δ_{ab} is different from Δ_{ac} and Δ_{bc} [3]. The latter two are similar to each other and to Δ_{ac} in ErMnO_3 (Fig. 3). The lowest-energy peak of orthorhombic NdMnO_3 at $\sim 1.2 \text{ eV}$ could be assigned to the ${}^5\Gamma_3 \rightarrow {}^5\Gamma_5$ transitions corresponding to the octahedral crystal field splitting Δ_o , in a good agreement with crystal field splitting in hexagonal ErMnO_3 . The common feature of the dielectric function spectra of several manganites is the wide band at $3.5\text{--}4.0 \text{ eV}$, which in the present model is assigned to charge transfer transitions with a polarization being opposite to that of $d\text{--}d$ transitions ${}^5\Gamma_1 \rightarrow {}^5\Gamma_5$ developed for $e\parallel a$. As compared to the data for NdMnO_3 [3], a particular feature of ErMnO_3 is a strong peak in the energy loss function spectra corresponding to the ${}^5\Gamma_1 \rightarrow {}^5\Gamma_5$ transitions.

The $f\text{--}f$ transitions in NdMnO_3 [3] as well as in ErMnO_3 (Fig. 4) correspond to those in other rare earth compounds [7].

4. Conclusions

Experimental data and their analysis have shown that common features in optical spectra of both hexagonal and perovskite manganites is a higher-energy ($3.5\text{--}4.0 \text{ eV}$) peak, which can be attributed to the charge transfer transitions. The fine spectral structure at lower energies ($1\text{--}2.6 \text{ eV}$) can be assigned to the optical transitions between the states originated from $3d^4$ levels of Mn^{3+} which are split in octahedral and trigonal bipyramidal crystal fields in perovskite and hexagonal manganites, respectively. A particular feature of ErMnO_3 is a strong peak at $\sim 1.6 \text{ eV}$. The $f\text{--}f$ transitions in manganites correspond to those obtained in other rare earth compounds.

Acknowledgements

The work was partially supported by the EU project PHOREMOST (N 511616) and Danish Technical Research Council.

References

- [1] J.M.D. Coey, M. Viret, and S. von Molnár, Mixed-valence manganites, *Adv. Phys.* **48**, 167–293 (1999).
- [2] G.A. Smolenskii and I.E. Chupis, Ferroelectromagnets, *Sov. Phys. Usp.* **25**, 475–493 (1982).
- [3] G.J. Babonas, A. Reza, R. Szymczak, M. Baran, S. Shiryaev, J. Fink-Finowicki, and H. Szymczak, Ellipsometric studies of NdMnO_3 single crystals, *Acta Phys. Pol. A* **105**, 197–208 (2004).
- [4] C. Degenhart, M. Fiebig, D. Fröhlich, Th. Lottermoser, and R.V. Pisarev, Nonlinear optical spectroscopy of electronic transitions in hexagonal manganites, *Appl. Phys. B* **73**, 139–144 (2001).
- [5] B.B. Van Aken, A. Meetsma, and T.T.M. Palstra, Hexagonal ErMnO_3 , *Acta Cryst.* **E57**, i38–i40 (2001).
- [6] S. Quezel-Ambrunaz, Parametres des manganites de terres rares Perovskites et structure magnetique du manganese dans MnPrO_3 et MnNdO_3 par diffraction neutronique, *Bull. Soc. Franc. Mineral. Crist.* **91**, 339–343 (1968).
- [7] G.H. Dieke, *Spectra and Energy Levels of Rare Earth Ions in Crystals* (Interscience Publishers, New York, 1968).
- [8] M. Qian, J. Dong, and Q. Zheng, Electronic structure of the ferroelectromagnet YmnO_3 , *Phys. Lett. A* **270**, 96–101 (2000).
- [9] J.E. Medvedeva, V.I. Anisimov, M.A. Korotin, O.N. Mryasov, and A.J. Freeman, The effect of Coulomb correlation and magnetic ordering on the electronic structure of two hexagonal phases of ferroelectromagnetic YMnO_3 , *J. Phys. Cond. Matter* **12**, 4947–4958 (2000).

ErMnO₃ MONOKRISTALŲ ELIPSOMETRINIAI TYRIMAIG.J. Babonas ^a, J.-C. Grivel ^b, A. Rėza ^{a,c}, R. Girkantaitė ^c^b *Puslaidininkų fizikos institutas, Vilnius, Lietuva*^a *Danijos technikos universitetas, Roskildė, Danija*^a *Vilniaus pedagoginis universitetas, Vilnius, Lietuva***Santrauka**

1–5 eV spektrų ruože, panaudojant fotometrinius elipsometrus, atlikti ErMnO₃ monokristalų elipsometriniai tyrimai. Eksperimentiniai elipsometriniai duomenys analizuoti remiantis vienašio kristalo modeliu. Pirmą kartą nustatyti ErMnO₃ dielektrinės funkcijos komponentų spektrai. Išnagrinėta dielektrinės funkcijos spektrų

smulkioji sandara ir aptarta optinių ypatumų kilmė, atsižvelgiant į galimus elektroninių sužadinių mechanizmus. Nustatyta, kad ErMnO₃ optinį atsaką sukelia nekeičiantys jonų Mn³⁺ ir Er³⁺ konfigūracijų, atitinkamai *d-d* ir *f-f*, šuoliai ir O(2*p*)→Mn(3*d*) šuoliai su krūvio pernaša. Palyginti ErMnO₃ ir kitų manganitų optiniai spektrai ir elektroninių juostų sandara.